This relationship has been investigated by Nachtrieb *et al.*[4] and Hudson and Hoffman[5] for self diffusion in lead and found to hold only for pressures below about 12 kbar. It is concluded inasmuch as the experimental data for $\ln D$ versus T_m/T as shown in Fig. 4 have about the same scatter as the isobar data for $\ln D$ versus $1/T$ from Fig. 2 that within the experimental error a relation of the form of Eq. (6) is valid to 40 kbar for the diffusion of Ag into Pb. A least-squares analysis of the data of Fig. 4 yields a value of 15.3 kcal/mole for $\Delta H(0)$ from Eq. (6) in good agreement with Seith and Keil's[15] value of 15.2 kcal/mole. It is noted, however, that although the high-pressure data have about the same slope it predominately falls below the Seith and Keil[15] data. This is not surprising in terms of the proposed mechanism since the vacancy contribution to the diffusion disappears as the pressure increases.

The error limits as indicated in Table I for the activation energy have been calculated from the rms deviation between the experimental points and the curves of Fig. 2. The error limits for D_0 and the activation volumes ΔV as shown in Tables I and II have been estimated by relating them through Eqs. (3) and (4) to the errors in ΔH.

PHYSICAL REVIEW VOLUME 139, NUMBER 5A 30 AUGUST 1965

High-Field Magnetoresistance of Rhenium

W. A. Reed, E. Fawcett, and R. R. Soden
Bell Telephone Laboratories, Murray Hill, New Jersey
(Received 14 April 1965)

High-field magnetoresistance measurements show that rhenium is a compensated metal whose Fermi surface supports three sets of open orbits. One set, which dominates the behavior of the magnetoresistance, occurs on a nearly cylindrical electron surface whose axis is along [0001]. The mobility of these electrons is an ord er of magnitude less than that of the other carriers. A second set of open orbits, directed along $\langle 10\bar{1}0\rangle$ and res ulting from magnetic breakdown, is seen only in fields greater than about 30 kG. A third set, also directed along [0001], occurs on one of the sheets of the Fermi surface supporting the $\langle 10\bar{1}0\rangle$-directed orbits, resulting in two-dimensional regions of aperiodic open orbits centered on the $\langle 11\bar{2}0\rangle$ axes.

1. INTRODUCTION

THE galvanomagnetic properties of a metal in the high-field region, where the effect of collisions on the motion of the current carriers is small compared with the effect of the magnetic field, can provide direct information about its electronic structure. Lifshitz, Azbel' and Kaganov[1] showed in particular that the variation of the field dependence of the galvanomagnetic properties is independent of the collision processes in the high-field region and is governed solely by geometric features of the Fermi surface of the metal.

The high-field region is defined formally by the inequality,

$$\omega_c\bar{\tau}\gg 1, \tag{1}$$

which must be satisfied for *all* the carriers. In Eq. (1), ω_c is the cyclotron frequency,

$$\omega_c = eB/m^*c, \tag{2}$$

of a carrier of cyclotron mass m^* and charge e moving in its cyclotron orbit in the magnetic field B, and $\bar{\tau}$ is an average around the orbit of the relaxation time characterizing the collision and scattering of the carrier. For a given magnetic field, the high-field region can be achieved by increasing $\bar{\tau}$. This is accomplished by using a high-purity sample of the metal at a low temperature to reduce the scattering of the carriers by impurities and lattice vibrations.

For a given metal, the residual resistance ratio,

$$\mathrm{RRR} = R_{RT}/R_{4.2^\circ\mathrm{K}} = \rho_{RT}/\rho_{4.2^\circ\mathrm{K}}, \tag{3}$$

i.e., the ratio of the resistance R, and therefore the resistivity ρ, of a sample at room temperature ($\mathrm{RT}\approx 295^\circ\mathrm{K}$) and at 4.2°K, is a useful criterion for comparing the purity and perfection of different samples. ρ_{RT} is determined almost entirely by the scattering of the carriers by lattice vibrations and is almost independent of the impurity content of the metal sample, whereas $\rho_{4.2^\circ\mathrm{K}}$ is determined almost entirely by the scattering of the carriers by impurities and physical defects. Since ρ is inversely proportional to $\bar{\tau}$, RRR is a direct measure of the value of $\bar{\tau}$ for the sample at 4.2°K.

We describe in this paper measurements of the anisotropy and field dependence of the magnetoresistance of rhenium at 4.2°K. We employed one set of samples with current directions **J** oriented along the three major symmetry axes of this hcp metal and having values of RRR from about 1000 to 7000, and another set, similarly oriented, but having values of RRR from about 25 000 to 43 000.

Following an account of the experimental procedure

[1] I. M. Lifshitz, M. Ya Azbel', and M. I. Kaganov, Zh. Eksperim. i Teor. Fiz. **31**, 63 (1956) [English transl.: Soviet Phys.—JETP 4, 41 (1957)].

in Sec. 2, we describe in Sec. 3 the experimental results in the "medium-field" region, which we define by the criterion $\omega_c\bar{\tau}\sim 1$. In this region the magnetoresistance (measured on the set of samples of lower RRR) exhibits an unusual dependence on the magnetic field[2] for most directions of **B** and **J**. As the field increases, the magnetoresistance initially behaves as if it were going to saturate, but then the field-dependence curve goes through a point of inflection and increases more rapidly at higher fields until it approaches a quadratic power law.[3] We show by means of a simple model that the inflection can result from a large difference between the mobilities of the carriers on different sheets of the Fermi surface, one of which is open along the hexagonal axis. We also make a comparison of the magnetoresistance of the samples of higher RRR in fields up to 100 kG with the magnetoresistance in the medium field region and find that Kohler's rule is obeyed.

In Sec. 4 we describe the measurements up to 100 kG on the samples of both low and high RRR. These measurements, in which $\omega_c\bar{\tau}\gg 1$ for all carriers, show that, in addition to the open orbits directed along the hexagonal axis whose effects we describe in Sec. 3, the Fermi surface of rhenium also supports two sets of open orbits not seen in the medium-field region. One set is directed along the $\langle 10\bar{1}0\rangle$ axes and exists whenever the field is in a $\{10\bar{1}0\}$ plane.[4] The other is directed along the [0001] axis and exists for all directions of the field in the (0001) plane.[5] We conclude that these two sets of open orbits occur on the same sheet of Fermi surface since a two-dimensional region where the magnetoresistance saturates[6] is observed around the $\langle 11\bar{2}0\rangle$ axes. The saturating magnetoresistance associated with the $\langle 10\bar{1}0\rangle$-directed open orbits does not obey Kohler's rule, but instead scales with RRR in a manner corresponding to magnetic breakdown.

2. EXPERIMENTAL PROCEDURE

The rhenium was purified by electron beam float-zoning using compressed and sintered rods of the powdered metal.[7] After several passes of the molten zone, the crystals of rhenium were seeded to grow with their axes within 1° of a symmetry axis. The purity of the single crystals was checked by measuring their RRR, which in the case of the higher purity samples was required to be greater than 25 000. The lower purity samples were prepared in a similar manner but from less pure starting material.

TABLE I. Orientation and residual resistance ratio (RRR) of rhenium samples.

Sample	Orientation	RRR
Re 208	$[10\bar{1}0]$	920
Re 210	[0001]	950
Re 215	$[11\bar{2}0]$	3960
Re 382	$[11\bar{2}0]$	6770
Re 409	$[11\bar{2}0]$	43 300
Re 421	[0001]	25 800
Re 424	$[10\bar{1}0]$	24 000

A cylindrical sample about 15 mm long by 2 mm diam was spark-cut from each single crystal. Three pairs of mutually perpendicular potential leads were soldered to each sample so that all components of the electric field could be measured. The Hall (transverse) leads were placed in a plane perpendicular to the sample axis, and the magnetoresistance leads were placed above and below the Hall leads separated by about 6 mm. The orientation and residual resistance ratio of each sample was checked after cutting and mounting with potential leads, and is given in Table I.

For the measurements up to 18 kG the sample was mounted in an assembly so constructed that it can be rotated ±5° about one horizontal axis and ±90° about the other perpendicular horizontal axis. In this way the sample can be accurately aligned in the magnetic field and tilted from a vertical to a horizontal position while immersed in liquid helium. For any tilt angle φ between the sample axis and the vertical, the Varian magnet can be rotated about a vertical axis to make any required angle θ between the magnetic field and a fiducial direction in the horizontal plane. The potentials

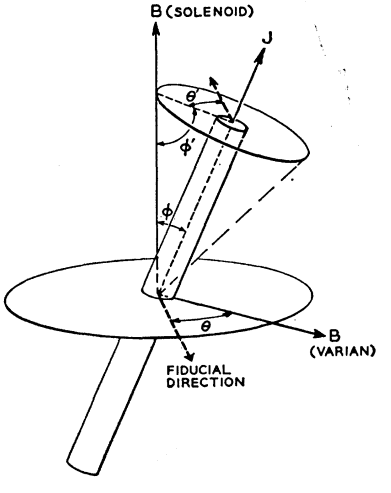

FIG. 1. Angular coordinates of the magnetic field **B** relative to the sample for the two experimental geometries.

[2] In a weakly magnetic metal like rhenium the difference between the magnetic induction **B** and the applied magnetic field $\mathbf{H}_0$ is so small that for our purposes we consider $\mathbf{B}=\mathbf{H}_0$, and for convenience we use the symbol **B** for both.

[3] W. A. Reed and E. Fawcett, Bull. Am. Phys. Soc. **7**, 478 (1962).

[4] N. E. Alekseevskii, V. S. Egorov, and B. N. Kazak, Zh. Eksperim. i Teor. Fiz. **44**, 1116 (1963) [English transl.: Soviet Phys.—JETP **17**, 752 (1963)].

[5] E. Fawcett and W. A. Reed, *Proceedings of the International Conference on Low Temperature Physics 1964* (to be published).

[6] I. M. Lifshitz and V. G. Peschanskii, Zh. Eksperim. i Teor. Fiz. **35**, 1251 (1958) [English transl.: Soviet Physics—JETP **8**, 875 (1958)].

[7] R. R. Soden, G. F. Brennert, and E. Buehler, J. Elec. Soc. **112**, 77 (1965).

were measured and the data reduced and plotted automatically by use of a system described by Reed and Brennert.[8]

The measurements up to 100 kG were made in a Bitter solenoid magnet. To recover the degree of freedom lost by the inability to rotate the magnetic field, a more elaborate assembly was used with the solenoid which permits the sample to be either tilted $\pm 90°$ about a horizontal axis or rotated $\pm 180°$ about its own axis.[9] The angular coordinates describing the orientation of the magnetic field relative to the sample in this case are the tilt angle φ' between the sample axis and the horizontal plane, and the sample rotation angle θ'. The two sets of angular coordinates corresponding to the two experimental geometries are illustrated in Fig. 1. The transverse magnetoresistance is measured when $\varphi=0$ or $\varphi'=0$ and in this case $\theta\equiv\theta'$. For equal but nonzero values of φ and φ', the directions of **B** corresponding to equal values of θ and θ' are not equivalent for the two geometries.

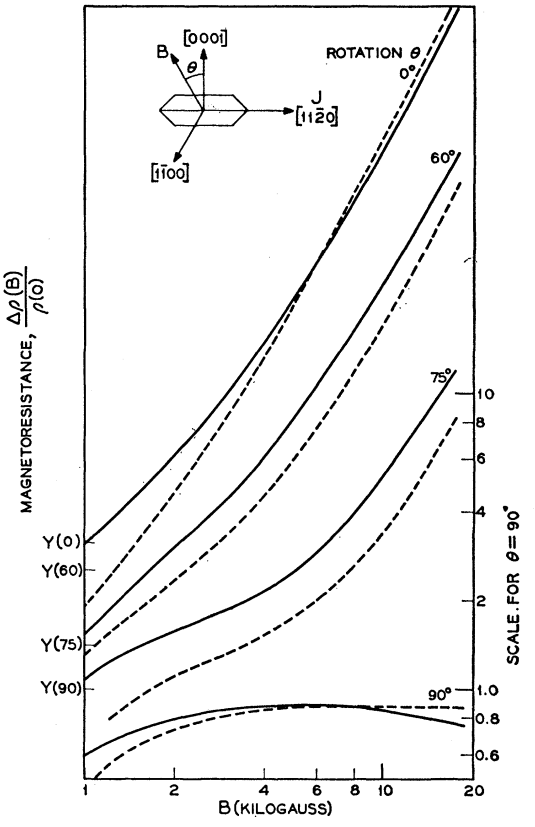

FIG. 2. Magnetoresistance of rhenium. The continuous curves show the field dependence of the transverse magnetoresistance ($\varphi=0°$) of sample Re 215 for several values of the rotation angle θ measured from the [0001] axis. The points $Y(\theta)$ on the left-hand ordinate axis show for each value of θ where the magnetoresistance is equal to 1.0, and the right-hand ordinate scale should be shifted accordingly. The dashed curves correspond to the cylinder-sphere model of the Fermi surface described in the text.

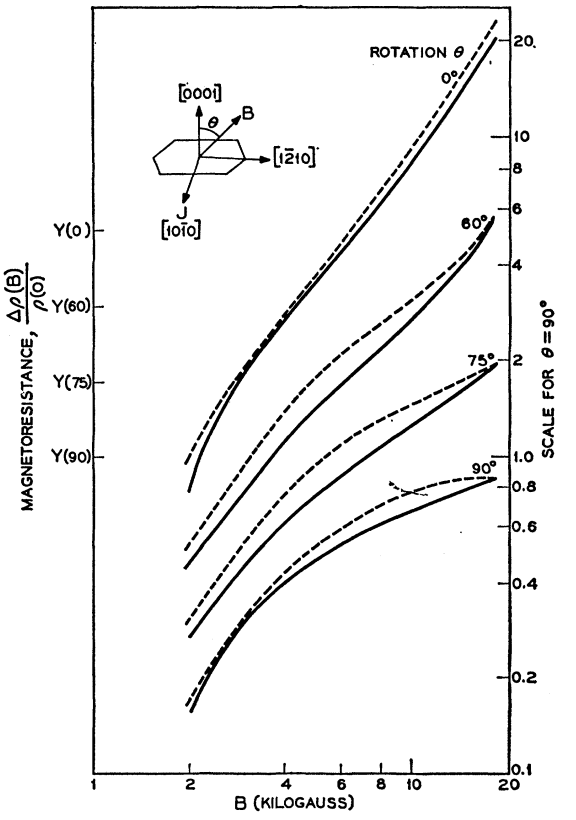

FIG. 3. Magnetoresistance of rhenium. The continuous curves show the field dependence of the transverse magnetoresistance ($\varphi=0°$) of sample Re 208 for several values of the rotation angle θ measured from the [0001] axis. The points $Y(\theta)$ on the left-hand ordinate axis show for each value of θ where the magnetoresistance is equal to 1.0 and the right-hand ordinate scale should be shifted accordingly. The dashed curves correspond to the cylinder-spheres model of the Fermi surface described in the text.

3. MEDIUM FIELD REGION

A. Experimental

The continuous curves in Figs. 2 and 3 show the measured field dependence of the transverse magnetoresistance in fields up to 18 kG at a temperature of 4.2°K for samples Re 215 and Re 208, which have their axes in the basal plane. Sample Re 210, with its axis along the hexagonal axis, has an almost isotropic transverse magnetoresistance at 18 kOe and its field-dependence is everywhere similar to the curve $\theta=0°$, in Fig. 3 for sample Re 208, which has about the same RRR (Table I).

For each of the three samples, the magnetoresistance increases more rapidly than linearly with increasing field at the higher fields, except when **B** lies within about 10° of the basal plane ($\theta>80°$). When $\theta=90°$ in

[8] W. A. Reed and G. F. Brennert, Phys. Rev. **130**, 565 (1963).
[9] G. F. Brennert, W. A. Reed, and E. Fawcett, Rev. Sci. Instr. (to be published).

Figs. 2 and 3 the magnetoresistance is very low and approaches saturation,[10] which suggests that there is an open sheet of the Fermi surface supporting open orbits directed along the hexagonal axis when **B** is in the basal plane. This saturation and the approach of the transverse magnetoresistance to a quadratic field dependence for sample Re 210 with **J** along the hexagonal axis is consistent with the behavior of the magnetoresistance of a metal in the high-field region where **B** is in a direction producing open orbits on its Fermi surface. In this case the resistivity for **J** in the x-y plane perpendicular to **B** making an angle α with the open x direction is

$$\rho_{\alpha\alpha}=(C_{xx}^{0}+C_{xx}^{2}B^{2})\cos^{2}\alpha+C_{yy}^{0}\sin^{2}\alpha, \tag{4}$$

where C_{xx}^{0}, C_{xx}^{2} and C_{yy}^{0} are field-independent coefficients.[6] We conclude that one sheet of the Fermi surface of rhenium supports a broad band of open orbits along the hexagonal axis when **B** is in the basal plane. The characteristics of this sheet are discussed further in Sec. 3B.

The fact that for most directions of the field and current the magnetoresistance increases faster than linearly at the higher fields (and approaches a quadratic power law when $B\sim 100$ kG) shows that rhenium is a compensated metal having equal numbers of holes and electrons. This result is expected for a metal with a hcp structure and, therefore, with two atoms per unit cell.[11]

At the lower fields the curves in Figs. 2 and 3 show an unusual behavior. The field dependence of the magnetoresistance first begins at low fields to approach saturation, and then at higher fields turns upwards. The point of inflection moves to higher fields as θ increases and disappears altogether when $\theta=90°$ and **B** is in the basal plane.

B. Model of the Fermi Surface

The unusual field-dependence of the magnetoresistance of rhenium can be explained by means of a simple model of its Fermi surface. We represent the open sheet by a cylindrical electron surface, open along the hexagonal axis, with carriers having a mobility, $\mu_e^{0}\cos\psi$, where ψ is the angle between **B** and the open direction. The rest of the Fermi surface, consisting in general of both electron and hole sheets, must contain a *net* number of holes equal to the number of electrons in the open sheet for the model to be compensated. We assume that these other sheets are closed and represent them by two spherical surfaces containing n_e^{c} electrons and n_h^{c} holes such that

$$n_e^{c}+n_e^{0}=n_h^{c}, \tag{5}$$

n_e^{0} being the number of electrons per unit cell in the open sheet. We arbitrarily assume that the electrons and holes in the spherical surfaces have the same mobility $\mu_{h,e}^{c}$ which is about an order of magnitude larger than μ_e^{0}.

For this model the high mobility carriers on the spherical surfaces enter the high-field region when B reaches a value such that $\mu_{h,e}^{c}B=1$, this value of B being independent of ψ. But the electrons in the open surface do not enter the high-field region until B is increased by a factor $\mu_{h,e}^{c}/\mu_e^{0}\cos\psi$. At intermediate fields the model behaves like an uncompensated metal and the magnetoresistance approaches saturation, because only the spherical surfaces are in the high-field region. At higher fields its magnetoresistance must eventually approach the quadratic field-dependence characteristic of a compensated metal, except when **B** is perpendicular to the axis of the cylinder and there are open orbits perpendicular to the current direction. Therefore, the field-dependence curve must turn upwards at higher fields, giving rise to a point of inflection which moves to higher fields like $1/\cos\psi$ as ψ increases.

We describe the model formally by writing the conductivity tensor for the two spherical surfaces:

$$\sigma_{ij}^{c}=\frac{\sigma_{h+e}^{c}}{1+t_{h,e}^{c2}}\begin{Vmatrix}1 & Kt_{h,e}^{c} & 0\\ -Kt_{h,e}^{c} & 1 & 0\\ 0 & 0 & 1+t_{h,e}^{c2}\end{Vmatrix} \tag{6}$$

where σ_{h+e}^{c} is the sum of the contributions of the spherical surfaces to the conductivity in zero field, and we write

$$t_{h,e}^{c}\equiv|\omega_c\tau|_{h,e}^{c}\equiv\mu_{h,e}^{c}B \tag{7}$$

and

$$K=\frac{n_h^{c}-n_e^{c}}{n_h^{c}+n_e^{c}}=\frac{n_e^{0}}{n_h^{c}+n_e^{c}}. \tag{8}$$

The conductivity tensor for the open cylindrical electron surface is

$$\sigma_{ij}^{0}=\frac{\sigma_e^{0}}{1+t_e^{02}\cos^{2}\psi}\begin{Vmatrix}0 & -t_e^{0}\cos\psi & 0\\ t_e^{0}\cos\psi & 1 & 0\\ 0 & 0 & 0\end{Vmatrix}, \tag{9}$$

where we write

$$t_e^{0}\equiv|\omega_c\tau|_e^{0}\equiv\mu_e^{0}B. \tag{10}$$

In Eq. (9) we choose the z axis as the open direction (the hexagonal axis) making an angle ψ with **B**, and σ_e^{0} is the contribution of the cylindrical surface to the conductivity in zero field in the x-y plane.

[10] For sample Re 215, when $\theta=90°$, the magnetoresistance goes through a broad maximum as B increases; and when $B\gtrsim 6$ kG, it decreases with increasing B (Fig. 2). The two other samples of the same orientation show similar behavior and for Re 424 the magnetoresistance actually becomes negative at the higher fields. The explanation of this behavior is not known, but presumably the mechanism responsible for the negative magnetoresistance can only produce an appreciable effect when the magnetoresistance is very low.

[11] E. Fawcett and W. A. Reed, Phys. Rev. **131**, 2463 (1963).

If we define

$$R=\mu_e^0/\mu_{h,e}{}^c\equiv t_e^0/t_{h,e}{}^c \tag{11}$$

as the ratio of the mobility of the electrons on the cylindrical surface when $\psi=0°$ to the mobilities of the carriers on the spheres, we can write the zero-field conductivity σ in the basal plane,

$$\begin{aligned}\sigma&=e\{(n_e{}^c+n_h{}^c)\mu_{h,e}{}^c+n_e{}^0\mu_e{}^0\}\\&=(en_e{}^0\mu_{h,e}{}^c/K)(1+KR),\end{aligned} \tag{12}$$

by Eqs. (5), (8), and (11). A comparison of Eq. (12) with the equation,

$$\sigma=\sigma_{h+e}{}^c+\sigma_e{}^0, \tag{13}$$

gives

$$\sigma_{h+e}{}^c=\sigma/(1+KR),\quad \sigma_e{}^0=KR\sigma/(1+KR). \tag{14}$$

The parameters which can be varied to obtain the best fit to the experimental data are K, n_e^0 and R. For a given sample the measured conductivity σ in zero field at 4.2°K,[12] together with the mobility ratio R and the carrier number ratio K, determines $\sigma_{h+e}{}^c$ and $\sigma_e{}^0$ separately from Eq. (14). For a given value of B, n_e^0 then determines the values of $t_{h,e}{}^c$ and t_e^0, since from Eqs. (7) and (8)

$$\sigma_{h+e}{}^c=\frac{e}{c}(n_e{}^c+n_h{}^c)\mu_{h,e}{}^c=\frac{e}{c}\frac{n_e{}^0}{K}\frac{t_{h,e}{}^c}{B}, \tag{15}$$

and from Eqs. (8) and (10)

$$\sigma_e{}^0=\frac{e}{c}n_e{}^0\mu_e{}^0=\frac{e}{c}\frac{n_e{}^0t_e{}^0}{B}. \tag{16}$$

We determine the total conductivity tensor by adding the tensors (6) and (9) for various values of ψ and then invert the conductivity tensor to obtain the resistivity tensor. To evaluate a field-dependence curve for a given value of ψ, we compute the resistivity tensor for various values of $t_{h,e}{}^c$, and obtain the corresponding values of B for the assumed values of K, n_e^0 and R from Eqs. (14) and (15):

$$B=\frac{n_e{}^0et_{h,e}{}^c}{K\sigma_{h+e}{}^c}=\frac{1+KR}{K\sigma}n_e{}^0et_{h,e}{}^c. \tag{17}$$

The procedure for determining the values of the parameters R, n_e^0 and K which best fit the experimental curves for the field dependence of the magnetoresistance is as follows. The asymptotic value of the saturating magnetoresistance is determined at $\theta=90°$ for the samples having their axes in the basal plane.[13] For the model the saturating magnetoresistance for $\psi=90°$[14] approaches in the limit of infinite field the value,

$$\frac{\Delta\rho(\infty)}{\rho(0)}=\frac{\rho(\infty)-\rho(0)}{\rho(0)}=\frac{1+KR}{K^2+KR}-1. \tag{18}$$

Since $R<0.1$ and $K\lesssim 1$, we can neglect the term KR in both numerator and denominator of Eq. (18) and equate this expression to the measured asymptotic value to obtain a rough approximation to K.

The ratio of the field at which the magnetoresistance first begins to saturate to the field at the inflection point is a rough measure of $R/\cos\psi$. It is impractical to measure this ratio accurately, but the best value of R can be obtained by optimizing the fit between the *shape* of the computed field-dependence curves for the model in the medium-field region and the experimental curves of Figs. 2 and 3. The computed field-dependence curves show the magnetoresistance as a function of $t_{h,e}{}^c$ and the conversion factor, obtained by comparing with the experimental curves showing the magnetoresistance as a function of B, gives n_e^0 by Eq. (17).

The model makes no distinction between samples having different current directions in the basal plane, but we fit it to data from the rhenium samples with their axes along the different two-fold symmetry axes. These data are similar but not identical, so that the optimum set of values of K, n_e^0, and R is necessarily a compromise. These values are given in Table II, and the corresponding curves showing the magnetoresistance as a function of the transverse field are represented by the dashed lines in Figs. 2 and 3. For these values of the parameters, the value of $(\omega_c\tau)_{e,h}{}^c$ for a sample having RRR=10 000 in a field of 100 kG is 370 and the values of $n_e{}^c$ and $n_h{}^c$ are 0.04 and 0.22 carriers per cell, respectively. The value of R is thought to be accurate to within a factor of 2, but the *numbers* of carriers in the different sheets, and thus the values of $\omega_c\bar{\tau}$, may differ between the real metal and the model by a large factor.

According to the model, the magnetoresistance, when the field is rotated in the $(11\bar{2}0)$ plane, should vary as $\cos^2\theta$ in the high-field region. This result follows directly from the assumed cylindrical nature of the open electron surface and is in good agreement with the observed

TABLE II. Parameters for the cylinder-sphere model of the Fermi surface of rhenium.

Number per unit cell of electrons in the open sheet:	$n_e^0=0.18$
Number ration [Eq. (8)]:	$K=0.71$
Mobility ratio [Eq. (11)]:	$R=13$

[12] The conductivity σ is not measured directly since the sample cross section is usually irregular and cannot be measured accurately. Instead the value of σ at room temperature is assumed to equal that of polycrystalline rhenium ($\sigma_{RT}=5.4\times10^{-4}\ \Omega^{-1}\ \mathrm{cm}^{-1}$), and the value of σ at 4.2°K is found by multiplying σ_{RT} by RRR.

[13] An asymptotic value $\Delta\rho(\infty)/\rho(0)=0.9$ is adopted for the saturating magnetoresistance at $\theta=90°$. This corresponds roughly to the *maximum* value of the magnetoresistance for the curve, $\theta=90°$, of Fig. 2, and the asymptotic value for the curve, $\theta=90°$, of Fig. 3.

[14] For the samples having their axes in the basal plane, $\psi\equiv\theta$ when $\varphi=0°$, since the rotation angle θ is measured from the hexagonal axis (see Fig. 1).

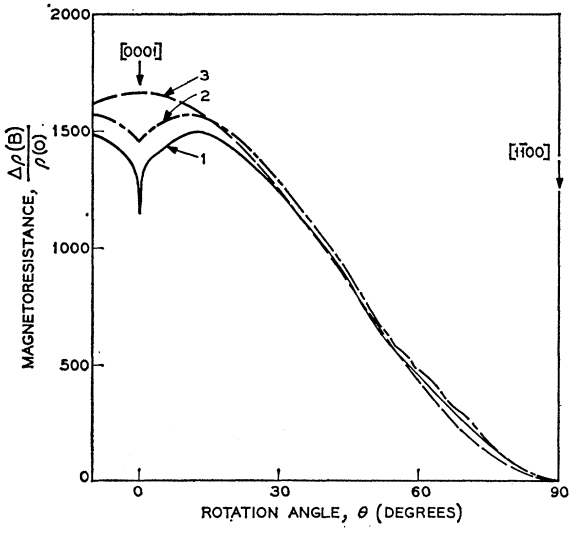

FIG. 4. Magnetoresistance of rhenium. Curve 1 shows the transverse magnetoresistance ($\varphi=0°$) of sample Re 215 in a field, $B=90$ kG, as a function of the rotation angle θ measured from the [0001] axis. The transverse magnetoresistance of sample Re 409, which has the same orientation, in a field, $B=18$ kG, is scaled down by the factor given by Eq. (24) and shown by curve 2. Curve 3 shows the function, $1670\cos^2\theta$, which closely fits the experimental data except for $\theta\sim0°$.

anisotropy of the magnetoresistance shown in Fig. 4 except when the field is near the hexagonal axis where effects resulting from open orbits in the basal plane are observed (see Sec. 4).

However, this simple model is not intended to be an accurate description of the Fermi surface of rhenium. There is no reason to suppose for example that the closed sheets of the Fermi surface are spherical, this assumption having been made only to render the model tractable analytically. However, the good agreement of the $\cos^2\theta$ dependence of the model to the experimental data at the higher fields leads us to believe that the open sheet approximates to a high degree a circular cylinder. The model also demonstrates that the physical explanation of the inflection in the field dependence of the magnetoresistance is the difference in the mobility of the carriers on different sheets of the Fermi surface.

C. Hall and Transverse Even Voltages

For the model of a cylinder and two spheres, the sign of the Hall voltage in the high-field region is determined by the relative mobilities and numbers of carriers in the electron and hole sheets. The Hall term of the resistivity tensor when **B** is along the hexagonal axis ($\psi=0°$) approaches in the limit of infinite fields the value,

$$\rho_{12}(\infty)=\frac{K(1+KR)(1-R^2)}{(R+K)^2}\frac{t_{h,e}}{\sigma}=\frac{K(1+KR)(1-R^2)}{(R+K)^2}\frac{\mu_{h,e}B}{\sigma}. \quad (19)$$

Since $R\ll1$, corresponding to the much lower mobility of the electrons on the cylindrical surface than of the electrons and holes on the two spheres, the Hall term is positive. When $\psi>0°$ the mobility $\mu_e{}^0\cos\psi$ of the electron on the cylindrical surface is even smaller, so that the Hall term is always positive.

We have not made a thorough experimental study of the transverse terms in the resistivity of rhenium, but the measured values of the Hall coefficient in the high-field region are found to be positive for several samples. We therefore conclude that the low-mobility carriers on the cylindrical surface are electrons.

D. Magnetic Breakdown

Falicov and Sievert[15] show that under conditions of magnetic breakdown, when electrons (or holes) describe trajectories in the magnetic field which connect different sheets of the Fermi surface, there is an additional scattering mechanism associated with incoherent Bragg reflection. The effective relaxation time τ_{eff} when magnetic breakdown is complete may be written

$$1/\tau_{\text{eff}}=1/\tau+C\omega_0, \quad (20)$$

where τ is the relaxation time in zero field, C is a constant of order unity and ω_0 is the cyclotron frequency at the breakdown field.

The magnetoresistance in the high-field region for a model comprising two spherical surfaces containing equal numbers of electrons and holes approaches

$$\frac{\Delta\rho(\infty)}{\rho(0)}=(\omega_c\bar{\tau})_e(\omega_c\bar{\tau})_h=\left(\frac{e}{c}\right)^2\left(\frac{\bar{\tau}}{m^*}\right)_e\left(\frac{\bar{\tau}}{m^*}\right)_h B^2. \quad (21)$$

If magnetic breakdown over the whole electron sheet occurs at a field B_0, and the values of $\bar{\tau}_e$ and $\bar{\tau}_h$ are sufficiently high that the metal is well into the high-field region at B_0, i.e.,

$$\omega_0\bar{\tau}_e\sim\omega_0\bar{\tau}_h\gg1, \quad (22)$$

then by Eqs. (20) and (21) the magnetoresistance approaches a new asymptotic limit,

$$\frac{\Delta\rho(\infty)}{\rho(0)}=\left(\frac{e}{c}\right)^2\left(\frac{1/C\omega_0}{m^*}\right)_e\left(\frac{\bar{\tau}}{m^*}\right)_h B^2. \quad (23)$$

At a field above B_0 the magnetoresistance given by Eq. (23) is smaller than the value obtained by extrapolating Eq. (21) to the same field in the ratio,

$$1/C\omega_0\bar{\tau}_e.$$

The experimental data, however, rule out magnetic breakdown as the explanation of the inflection in the field dependence of the magnetoresistance. According to Eq. (23) the magnetoresistance in the high-field region under conditions of magnetic breakdown varies

[15] L. M. Falicov and P. R. Sievert, Phys. Rev. Letters **12**, 550 (1964); Phys. Rev. **138**, A88 (1965).

as $B^2/\rho(0)$ since $\bar{\tau}_h$ varies as $1/\rho(0)$, whereas under conditions of *no* breakdown the magnetoresistance obeys Kohler's rule and varies as $[B/\rho(0)]^2$.

To demonstrate that the measured magnetoresistance obeys Kohler's rule in the high-field region, we show in Fig. 4 data for two samples of the same orientation as the field rotates in the same crystal plane. The curve showing the anisotropy of the transverse magnetoresistance of Re 215 in a field $B=90$ kG (curve 1) corresponds to the rotation of B illustrated in the insert to Fig. 2. The corresponding curve for Re 409 in a field $B=18$ kG (curve 2) is scaled down by a factor

$$\left\{\frac{[B/\rho(0)]_{409}}{[B/\rho(0)]_{215}}\right\}^2=\left\{\frac{B_{409}}{B_{215}}\right\}^2\times\left(\frac{\mathrm{RRR}_{409}}{\mathrm{RRR}_{215}}\right)^2$$

$$=\left(\frac{18}{90}\right)^2\times\left(\frac{43300}{3960}\right)^2=4.8, \quad (24)$$

where we use the values of RRR in Table I and the relation between RRR and $\rho_{RT}/\rho_{4.2°K}$ given by Eq. (3). The shape of the anisotropy curve is similar for the two samples and the magnetoresistance can be represented roughly by the function, $1670\cos^2\theta$, except when **B** is near the hexagonal axis ($\theta\sim0°$). The narrow minimum there results from open orbits in the basal plane, which we discuss in Sec. 4. The magnitude of the magnetoresistance scales by the expected factor to within the experimental accuracy, which is determined mainly by the accuracy of measuring the very low value of $\rho(0)$ for Re 409, about $\pm10\%$.

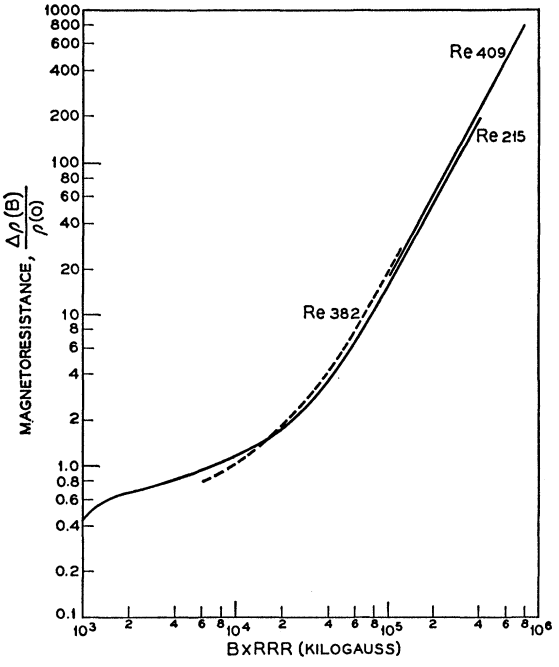

FIG. 5. Kohler diagram for rhenium. The transverse magnetoresistance ($\varphi=0°$) of the three $\langle11\bar{2}0\rangle$ samples for a rotation angle $\theta=75°$ measured from the [0001] axis, is plotted against $B\times$RRR. The measurements on Re 215 are taken up to $B=100$ kG, while the measurements on Re 382 and Re 409 are taken up to $B=18$ kG.

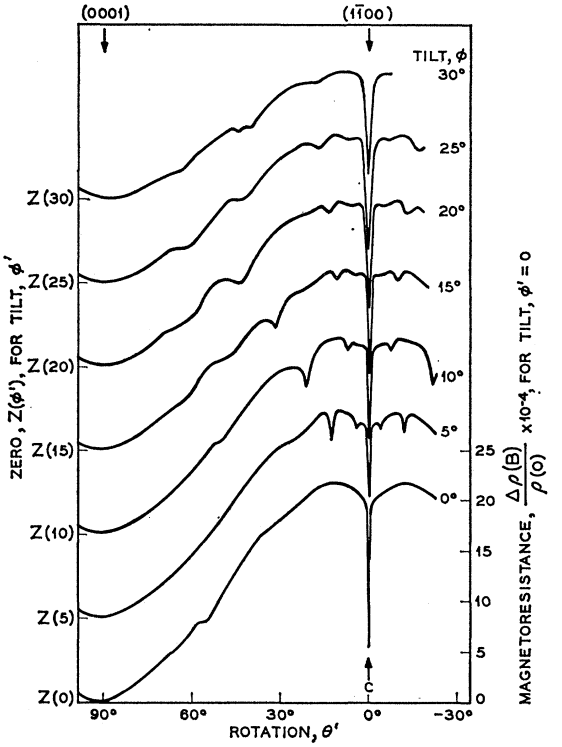

FIG. 6. Magnetoresistance of rhenium. The curves show the anisotropy of the magnetoresistance in a field of 100 kG of sample Re 424 as it is rotated about its $[10\bar{1}0]$ axis, which is inclined at various angles $(90-\varphi')$ to **B**. The points $Z(\varphi')$ on the left-hand ordinate axis show, for each value of φ', the origin for the magnetoresistance scale given on the right-hand ordinate axis, which should be shifted accordingly.

The experimental confirmation of Kohler's rule in the medium-field region is illustrated in Fig. 5 where the field-dependence curves for three different samples of the same orientation are plotted as a function of $B\times$RRR. The curves superimpose to within the experimental accuracy, showing that the magnetoresistance is indeed a function of this quantity.

4. HIGH-FIELD REGION

The anisotropy of the magnetoresistance of samples Re 424, Re 409 and Re 421 in a field of 100 kG is shown in Figs. 6, 7, and 8, respectively. These samples are the ones having higher RRR and they are oriented with their axes along the three symmetry axes (Table I). The three current directions and the locus of the field direction **B** as each sample is rotated about its axis at a tilt angle, $\varphi'=30°$ (Fig. 1), are shown in the stereogram of Fig. 10. The field-dependence of the magnetoresistance for several transverse directions of **B** is shown in Fig. 9.

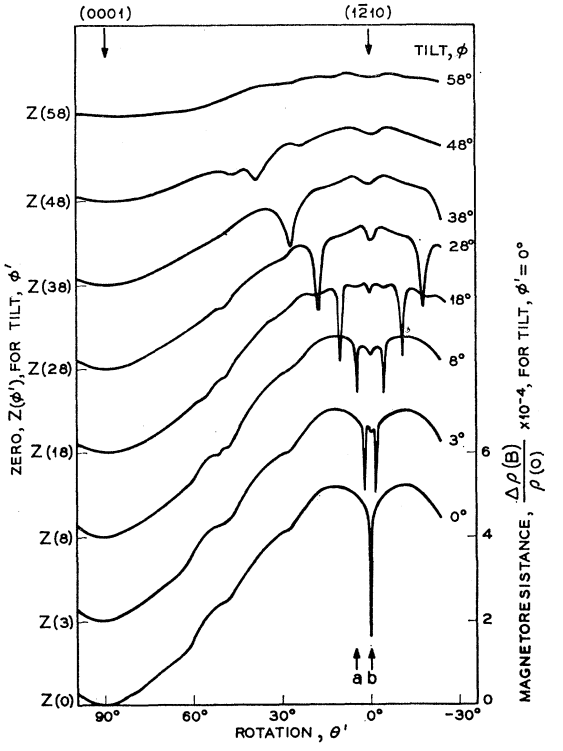

FIG. 7. Magnetoresistance of rhenium. The curves show the anisotropy of the magnetoresistance in a field of 100 kG of sample Re 409 as it is rotated about its [11$\bar{2}$0] axis, which is inclined at various angles $(90-\varphi')$ to **B**. The points $Z(\varphi')$ on the left-hand ordinate axis show, for each value of φ', the origin for the magnetoresistance scale given on the right-hand ordinate axis, which should be shifted accordingly.

For most field directions the field dependence of the transverse magnetoresistance approaches but does not quite achieve a quadratic power law. For example, if we write

$$\frac{\Delta\rho(B)}{\rho(0)}=\text{const}\ B^m, \tag{25}$$

the exponent m has the value 1.91 for the field-dependence curve labeled (a) in Fig. 9, corresponding to a field direction 5° away from the hexagonal axis of sample Re 424 (see Fig. 6). The value of m is 1.90 for the higher values of B on the curves for both Re 409 and Re 215 shown in Fig. 5, the field direction for these curves being 15° from the basal plane. These values of m are less than 2.00 by an amount significantly greater than the experimental accuracy, which is about $\pm 1\%$ for the measurements up to 18 kG and about $\pm 2\%$ for the measurements up to 100 kG. Other compensated metals have been observed to exhibit in the high-field region a field-dependence of their transverse magnetoresistance with $m \lesssim 2$, so that although the cause of these small discrepancies from the theoretical value of exactly two has not been explained,[16] we can nevertheless conclude with some confidence that rhenium is compensated.

When **B** lies in either the (0001) or {10$\bar{1}$0} planes the magnetoresistance may exhibit a saturating field-dependence, depending upon the direction of the current. For example, in Figs. 6 and 7 each curve shows the anisotropy of the magnetoresistance for a different value of the tilt angle φ', but they all have a broad deep minimum centered on $\theta'=90°$, where **B** lies in the (0001) plane. The magnetoresistance here saturates at a low value less than 10, i.e., at least four orders of magnitude smaller than the maximum value near $\theta'=10°$. We saw in Sec. 3 (cf. Fig. 4) that this behavior results from a band of open orbits on a nearly-cylindrical sheet of the Fermi surface with its axis along the hexagonal axis.

A. ⟨10$\bar{1}$0⟩ Open Orbits

In the case of the samples having their axes in the basal plane, there is a narrow minimum when **B** is along the hexagonal axis, i.e., at $\theta'=0°$, $\varphi'=0°$ in Figs. 6

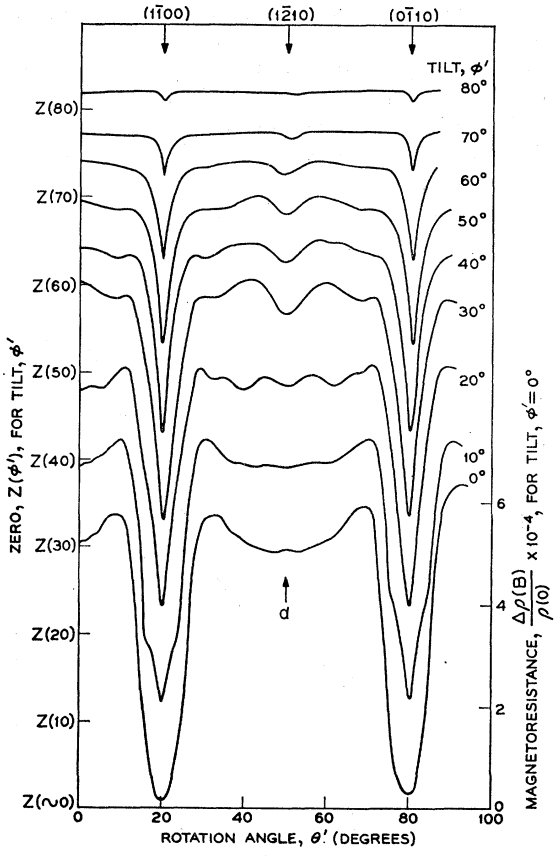

FIG. 8. Magnetoresistance of rhenium. The curves show the anisotropy of the magnetoresistance in a field of 100 kG of sample Re 421 as it is rotated about its [0001] axis, which is inclined at various angles $(90-\varphi')$ to **B**. The points $Z(\varphi')$ on the left-hand ordinate axis show, for each value of φ', the origin for the magnetoresistance scale given on the right-hand ordinate axis, which should be shifted accordingly.

[16] E. Fawcett, Advan. Phys. 13, 139 (1964).

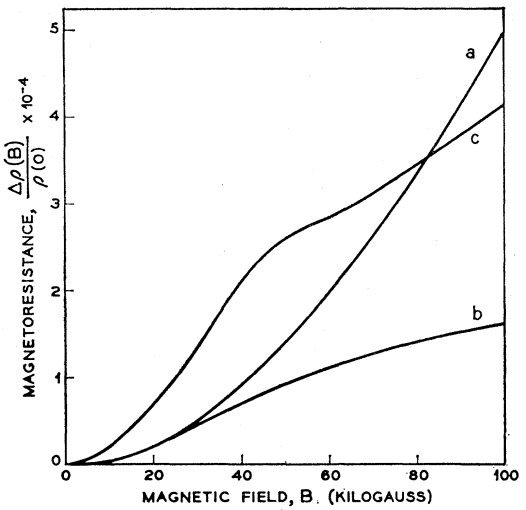

FIG. 9. Magnetoresistance of rhenium. The curves show the field dependence of the transverse magnetoresistance when **B** is in the directions indicated by the arrows labeled (a), (b) in Fig. 6, and (c) in Fig. 7.

and 7. The corresponding field-dependence curves, which are illustrated in Fig. 9 (curves b and c), show that these minima are associated with an approach to saturation of the magnetoresistance starting at $B\sim 30$ kG. As the tilt angle φ' is increased from zero, this minimum in the anisotropy curves for the $[10\bar{1}0]$-axis sample Re 424 (Fig. 6) resolves into two minima symmetrically displaced from $\theta'=0°$ with a much shallower minimum remaining at $\theta'=0°$ in the $(1\bar{2}10)$ plane. For the $[11\bar{2}0]$-axis sample Re 409 (Fig. 7), the relatively deep minimum remains at $\theta'=0°$ where **B** lies in the $(1\bar{1}00)$ plane, while two pairs of symmetrically displaced minima appear and move away from $\theta'=0°$ as φ' is increased, the inner pair in the $\{11\bar{2}0\}$ planes being somewhat shallower than the center pair in the $\{10\bar{1}0\}$ planes.

In the anisotropy curves for the [0001]-axis sample Re 421 (Fig. 8) deep minima occur when **B** lies in a $\{10\bar{1}0\}$ plane. As φ' is increased these minima become narrower and less deep, but they are still quite distinct when $\varphi'=80°$ and the sample is only 10° from a longitudinal orientation with respect to the field. For some values of φ' the anisotropy curves in Fig. 8 also exhibit a minimum in the $(1\bar{2}10)$ plane. But this minimum is much shallower and the magnetoresistance always has a quadratic field-dependence at its center, whereas the magnetoresistance approaches saturation at the bottom of the minimum in the $\{10\bar{1}0\}$ plane for all values of φ' except $\varphi'=0°$ (see Fig. 11).

The deeper minima in the anisotropy curves of Figs. 6, 7, and 8 coincide within the experimental accuracy with the direction of **B** lying in the $\{10\bar{1}0\}$ planes and the (0001) plane, which are shown by continuous lines in the stereogram of Fig. 10. This suggests that the former result from open orbits along the $\langle 10\bar{1}0\rangle$ axes, which dominate the resistivity tensor and produce a magnetoresistance of the form given by Eq. (4). For example, the minima at $\theta'=0°$ in Fig. 7 are produced by open orbits along $[1\bar{1}00]$, which is perpendicular to the current direction $[11\bar{2}0]$, so that $\alpha=90°$ and the magnetoresistance saturates in agreement with Eq. (4). The outer pair of minima which appear in Fig. 7 when φ' is increased from zero are produced by open orbits along $[01\bar{1}0]$ and $[10\bar{1}0]$, but since $\alpha=30°$ the magnetoresistance still has a quadratic field-dependence at the bottom of these minima corresponding to the dominant term $C_{xx}{}^2B^2\cos^2\alpha$ in Eq. (4).

One might suspect that the inner pair of shallower minima in Fig. 7, which coincide with the $\{11\bar{2}0\}$ planes, likewise indicate the existence of open orbits along the $\langle 11\bar{2}0\rangle$ axes. But such open orbits would be along $[\bar{1}2\bar{1}0]$ when $\theta'=0°$ in Fig. 6, so that $\alpha=90°$, and according to Eq. (4) the magnetoresistance would saturate, whereas the magnetoresistance is found experimentally to have a quadratic field-dependence at the bottom of the shallow minimum at $\theta'=0°$ (except when $\theta'=0°$ and **B** is along the [0001] axis). We conclude that the shallower minima in Figs. 6, 7, and 8 which coincide with the $\{11\bar{2}0\}$ planes do not result from open orbits.

On the other hand the pair of minima symmetrically displaced from $\theta'=0°$ which appears in Fig. 7 when φ' is increased from zero provide further confirmation of the existence of open orbits along the $\langle 10\bar{1}0\rangle$ axes. In this case, $\alpha=60°$, so that in agreement with Eq. (4) the minima are deeper than the corresponding minima in Fig. 6 for which $\alpha=30°$. The magnetoresistance saturates at the bottom of the deep minima in Fig. 8 for all values of φ' except $\varphi'=0°$ (see Fig. 11), since for this sample the current is along the [0001] axis so that $\alpha=90°$ for open orbits along any of the $\langle 10\bar{1}0\rangle$ axes.

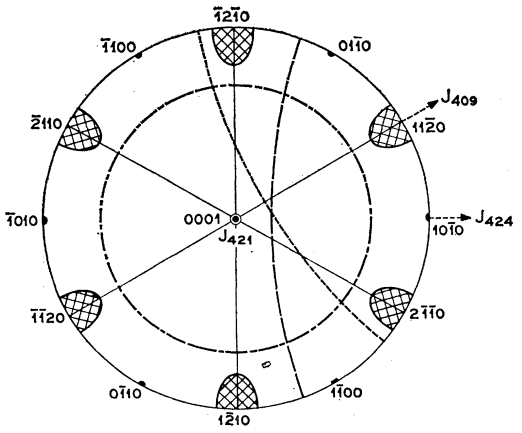

FIG. 10. Stereogram showing the current directions for the three samples of rhenium of higher purity. The broken lines show the motion of **B** as each sample is rotated about its axis for tilt angle, $\varphi'=20°$. The continuous lines show the directions of **B** where open orbits occur on a sheet of the Fermi surface. The shaded areas show the two-dimensional regions of open orbits.

B. ⟨0001⟩ Open Orbits

The insert in Fig. 11 shows the anisotropy of the magnetoresistance as **B** moves through the [11$\bar{2}$0] axis in the (1$\bar{1}$00) plane of the [0001] axis sample. This corresponds to moving the tilt angle φ' through zero for $\theta'=20°$ in Fig. 8. When $\varphi'=0$ the magnetoresistance is low and saturates, as shown by the lower field-dependence curve (e) in Fig. 11, corresponding to the existence of open orbits along [1$\bar{1}$00]. But a narrow maximum occurs at [11$\bar{2}$0], at the top of which the field-dependence of the magnetoresistance is roughly linear, as shown by curve (f) in Fig. 11.

The anisotropy of the magnetoresistance as the tilt angle φ' moves through zero for other values of θ' is shown in Fig. 12. A narrow maximum occurs at $\varphi'=0°$ for all values of θ', and when $\theta'>30°$ the field dependence of the magnetoresistance is quadratic both at the maximum and neighboring values of φ'. One would expect the existence of this maximum to reduce the depth of the minimum in the anisotropy curve for $\varphi'=0°$ in Fig. 8. But the maximum is so narrow that we can explain the absence of such an effect by supposing that the true value of φ' differs by a degree or so from zero for the observed anisotropy curve, since this is about the accuracy with which the sample can be oriented with respect to the magnetic field.

We attribute this narrow maximum to the effects of a *second* band of open orbits along the hexagonal axis, which occur only when **B** lies within a degree or so of the basal plane. The nearly cylindrical electron surface open along the hexagonal axis which we discussed in Sec. 3 is not adequate to account for this *narrow* maximum for *all* values of θ', since it merely tends to produce a *broad* maximum which is the counterpart of the broad minimum resulting from this surface when the current is perpendicular to the open direction (Fig. 4).

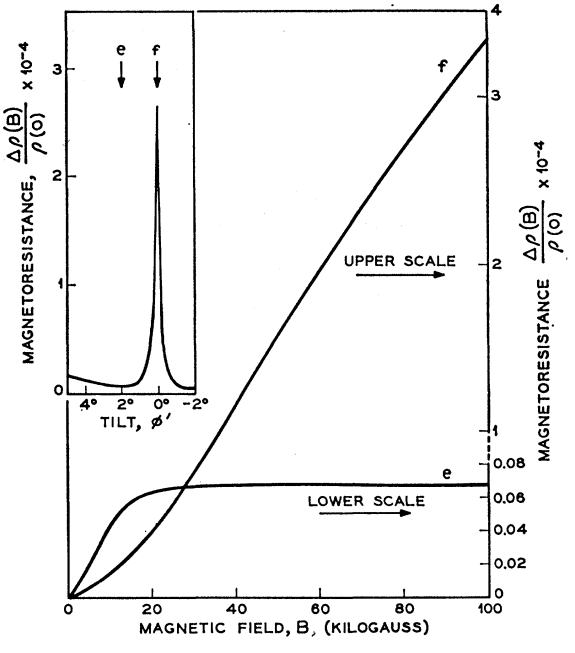

FIG. 11. Magnetoresistance of rhenium. The insert shows the anisotropy of the magnetoresistance of sample Re 421 as the tilt angle φ' is moved through zero for $\theta'=20$ in Fig. 8. The main diagram shows the field dependence of the magnetoresistance when **B** is in the directions indicated by the curves labeled e and f.

C. Two-Dimensional Region of Aperiodic Open Orbits

Since two bands of open orbits in nonparallel directions lead to a saturating transverse magnetoresistance,[6] the existence of the narrow maximum at the [11$\bar{2}$0] axis (i.e., in the curve $\theta'=20°$ of Fig. 12 at $\theta'=0°$) shows that [1$\bar{1}$00]-directed open orbits must vanish over an angular range roughly equal to that over which the [0001]-directed open orbits occur. This behavior suggests that these two bands of open orbits occur on the same sheet of the Fermi surface. The occurrence in the stereographic representation (Fig. 10) of two-dimensional regions centered on the ⟨11$\bar{2}$0⟩ axes where the magnetoresistance saturates is consistent with this conclusion, since *aperiodic* open orbits near the ⟨11$\bar{2}$0⟩ axes can only result from the intersection of the arms of the Fermi surface supporting the *periodic* open orbits along the ⟨10$\bar{1}$0⟩ axes and the [0001] axis.

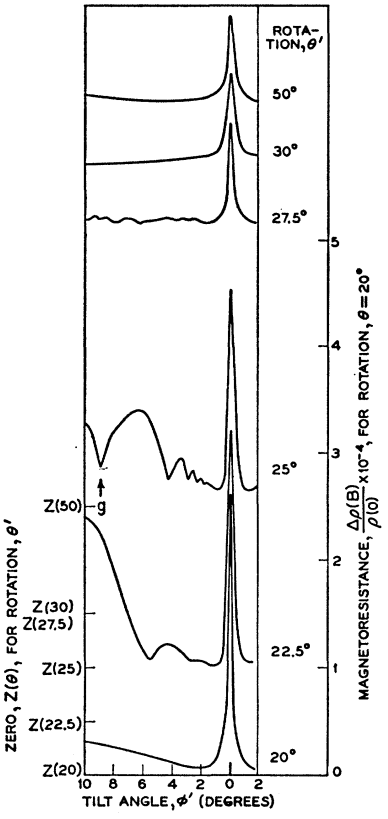

FIG. 12. Magnetoresistance or rhenium. The curves show the anisotropy of the magnetoresistance of sample Re 421 in a field of 90 kG as it is tilted so that **B** passes through the basal plane, where $\varphi'=0$, for various values of the rotation angle θ'. When $\theta'=20°$, **B** lies in the (1$\bar{1}$00) plane and the curve is identical to that shown in the insert of Fig. 11.

In Fig. 8 we interpret the steps on the sides of the deep minima for $\varphi'=10°$ to indicate approximately the extent of the two-dimensional region. In Fig. 12 the magnetoresistance saturates as far as 12° from the $[11\bar{2}0]$ axis at the point labeled g at $\varphi'=9°$ on the curve, $\theta'=25°$. In the stereogram of Fig. 10 the shaded areas centered on the $\langle 11\bar{2}0\rangle$ axes show the *approximate* extent of the regions where aperiodic open orbits occur.

D. Magnetic Breakdown

In Fig. 13 we show in a logarithmic plot the field dependence of the magnetoresistance of sample Re 409 with the field along the [0001] axis, i.e., in the direction labeled (c) in Fig. 7. We show also the field-dependence curves for the same field direction in samples Re 215 and Re 382, which have the same orientation as Re 409 but considerably lower values of RRR (see Table I). Figure 13 is a Kohler diagram in which the magnetoresistance is plotted against the product $B\times$RRR, so that according to Kohler's rule the three field-dependence curves should superimpose. Evidently Kohler's rule is not obeyed since the magnetoresistance of each sample approaches a different saturation value at the higher fields.

We attribute the observed behavior to the fact that the minimum which occurs for this field direction and sample orientation is produced by magnetic breakdown. According to Falicov and Sievert's theory,[15] when magnetic breakdown occurs and the magnetoresistance saturates in the high-field region, the saturation value is proportional to RRR. This result follows from Eq. (20), since when $C\omega_0$ is much greater than τ, the time τ_{eff} becomes independent of τ, the resistivity $\Delta\rho(B)$ becomes independent of $\rho(0)$, and the magnetoresistance $\Delta\rho(B)/\rho(0)(\sim\rho(B)/\rho(0))$ becomes proportional to RRR by Eq. (3).

In Fig. 13 the magnetoresistance of sample Re 409 begins to saturate when $B\times$RRR is about 2×10^6 kG, but the curve rises again at higher fields. This rise probably results from the extreme narrowness of the minimum in the magnetoresistance (see Fig. 7). The minimum is less than 0.5° wide and inhomogeneity of the magnetic field or microstructure in the sample of this magnitude[17] would introduce a nonsaturating component into the magnetoresistance. We believe that under better experimental conditions a sample of this orientation would have a saturating magnetoresistance of about 30 000 at the [0001] minimum. The [0001] minimum for sample Re 215 in a field of 90 kG is shown in curve (1) of Fig. 4. Evidently the field inhomogeneity or microstructure of this sample would introduce a much less significant error in the field-dependence curve than for sample Re 409. The same is true for sample

[17] We suspect that inhomogeneity of the field is more likely to cause this effect than microstructure since an x-ray analysis of a similar sample showed a spread in crystal orientation of less than 0.1°.

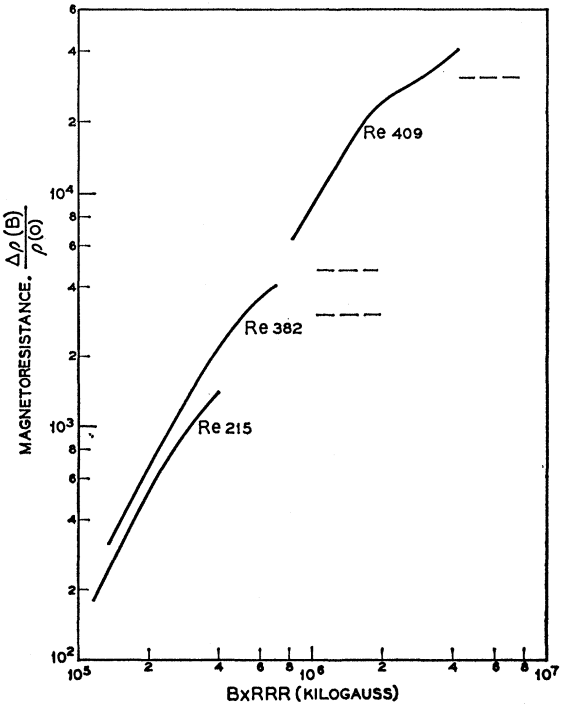

FIG. 13. Kohler diagram for rhenium. The magnetoresistance of the three $\langle 11\bar{2}0\rangle$ samples when B is directed along the [0001] minimum is plotted against $B\times$RRR. The measurements on all three samples are taken up to $B=100$ kG. The saturation value of the magnetoresistance discussed in the text is shown by the dashed line adjacent to each curve.

Re 382, but the shallowness of the minimum for this sample and for Re 215 results from the fact that even in a field of 100 kG the magnetoresistance of these samples of relatively low RRR is still rising towards the saturation value. If we assume that the minimum results from magnetic breakdown the saturation values of samples Re 282 and Re 215 would be about 4700 and 2750 when we scale the saturation value of 30 000 for sample Re 409 by the ratios of RRR from Table I according to Eq. (23). We see from Fig. 13 that the magnetoresistance at the minimum for samples Re 382 and Re 215 could plausibly be extrapolated to these saturation values. The evidence from Fig. 13 that the [0001] minimum results from magnetic breakdown is all the more convincing when we recall that, without such a mechanism, the magnetoresistance for the three samples would saturate at the *same* value according to Kohler's rule.

We can obtain a very rough estimate of the breakdown frequency ω_0 if we write $C=1$ in Eq. (20) and equate $\omega_0\tau$ to the saturation value 30 000 for sample Re 409. For this sample in a field of 100 kG the value of $\omega\tau$ is about 16 000, if we assume that the carriers producing the breakdown open orbits have a mobility roughly equal to that of the high-mobility carriers in the model of the Fermi surface described in Sec. 3, and scale ω_c with B and τ with RRR. If the effective mass

of these carriers is m^* and the free electron mass is m, we obtain a value,

$$\hbar\omega_0 = 2.17(m/m^*)\times 10^{-3} \text{ eV}. \quad (26)$$

A similar deviation from Kohler's rule is observed whenever **B** coincides with a $(10\bar{1}0)$ plane, and we conclude that the $\langle 10\bar{1}0\rangle$-directed open orbits are produced by magnetic breakdown. In fact for reasons of symmetry, no open orbits can exist when **B** coincides with the hexagonal axis. The saturation of the magnetoresistance for this field direction shown in Fig. 13 results from a change in the nature of the orbits in the breakdown region which destroys the compensation of the metal. A similar phenomenon is seen in zinc.[8] However, both our experimental measurements and the theoretical work of Falicov and Sievert[15] show that when saturation of the magnetoresistance results from breakdown, the saturation value scales with RRR both in the case of discompensation and open orbits.

In Fig. 12 the curve for $\theta' = 25°$ exhibits oscillations of the magnetoresistance periodic in $1/\varphi'$. These cannot be interpreted as Shubnikov–de Haas oscillations since the field dependence of the magnetoresistance is *not* oscillatory. A detailed explanation of these oscillations cannot be given without a knowledge of the connectivity and dimensions of the parts of the Fermi surface associated with the breakdown orbits. One possible explanation of this behavior is that in the two-dimensional region the aperiodic breakdown orbits consists of parts essentially parallel to the basal plane alternating with parts along the hexagonal axis. When $\varphi' \gg 1°$ each step along the hexagonal axis would correspond to a reciprocal lattice vector K_c, but at some critical angle, $\varphi' = \delta/K_c$, where δ is a dimension of the Fermi surface in the basal plane, the orbit would make a step of $2K_c$ along the hexagonal axis before breakdown into a direction parallel to the basal plane; then at $\varphi' = \delta/2K_c$, $\delta/3K_c$, etc. steps of $3K_c$, $4K_c \cdots$. At each critical angle, $\varphi' = \delta/nK_c$, the breakdown orbits would change; and since they dominate the magnetoresistance, the latter might be expected to oscillate.

CONCLUSIONS

Our study of the high-field magnetoresistance of rhenium provides information about some topological features of its Fermi surface. The nearly cylindrical electron surface with its axis along the hexagonal axis determines the main feature of the anisotropy of the magnetoresistance in both the medium-field and high-field regions, namely, the broad minimum seen in Fig. 4. The electrons on this surface have a mobility about an order of magnitude smaller than the carriers on the rest of the Fermi surface, and this high-mobility ratio gives rise to characteristic inflections in the field-dependence curves.

There are also open orbits directed along $\langle 10\bar{1}0\rangle$ which result from magnetic breakdown and are seen only in high magnetic fields. Another set of open orbits, also directed along [0001], occurs on one of the sheets of the Fermi surface supporting the $\langle 10\bar{1}0\rangle$-directed orbits, since aperiodic open orbits resulting from the intersection of the periodic orbits occur in a two-dimensional region of field directions near each of the $\langle 11\bar{2}0\rangle$ axes. The unusual oscillatory variation of the magnetoresistance when the field direction is varied within the two-dimensional region require further study when the connectivity of those parts of the Fermi surface associated with magnetic breakdown is better known.

A study of the de Haas–van Alphen effect in rhenium by Joseph and Thornsen[18] indicates that magnetic breakdown occurs between two sheets of the Fermi surface. Their data suggest that these two sheets are closed, and the breakdown orbits giving de Haas–van Alphen oscillations are necessarily closed, so that the open breakdown orbits which produce the saturating minima in the magnetoresistance may occur between other sheets of the Fermi surface. No de Haas-van Alphen oscillations corresponding to the nearly-cylindrical electron sheet have been observed, perhaps because the low mobility of these electrons correspond to a high effective mass which depresses the amplitude of the effect.

The shape and connectivity of the Fermi surface of rhenium are evidently quite complicated. No band structure calculation has as yet been done for rhenium; and without the guidance afforded by such a calculation, it is impracticable to construct the more complex features of the Fermi surface from the available experimental data.

ACKNOWLEDGMENTS

We are happy to acknowledge the able technical assistance of G. F. Brennert, R. D. Nafziger and H. W. Dail. We also want to thank Professor Leo Falicov for several discussions on the effects of magnetic breakdown. We are indebted to E. Buehler for growing some of the samples.

[18] A. S. Joseph and A. C. Thorsen, Phys. Rev. **133**, A1546 (1964).